Application of Dilatometry Testing and FE Simulation for Hot Forging Process

Uthaisangsuk V.

Department of Mechanical Engineering, Faculty of Engineering, King Mongkut's University of Technology Thonburi, Bangkok, Thailand

Apichat S.

Department of Tool and Material Engineering, Faculty of Engineering, King Mongkut's University of Technology Thonburi, Bangkok, Thailand

Chettaisong T.

Iron and Steel Institute of Thailand, Bangkok, Thailand

Abstract

Hot forging is a conventional forming process at elevated temperatures that is frequently used to produce bulk parts and components. By designing such hot forming processes FE simulations have been increasingly used. In this work, deformation behaviour of two common medium carbon steels was characterized at their hot-working temperature region by means of a deformation dilatometer machine. The effects of temperature, strain rate, and dynamic softening with respect to the recovery and recrystallization of material on the compressive flow stresses could be studied. In addition, phase transformation during continuous cooling after upsetting at high temperature was investigated for these steels. The flow curves and the Deformation Time-Temperature-Transformation (D-TTT) diagrams were determined using the determined experimental data. Subsequently, these material data could be applied for numerical FE simulations of industrial hot forging processes in order to optimize the parameters in the process. With a cellular automata (CA) model the calculation of microstructure evolution, dynamic recrystallized (DRX) grain size, and hardness of any selected areas in the forged parts after controlled cooling is possible.

Keywords*: Forging, Dilatometry, FE Simulation, D-TTT Diagram*

1 Introduction

Most of the industrial entrepreneurs in Thailand still show a lack of technology breakthrough to effectively predict and control the hot forming process. The process control is mainly based on experience from trial-and-error. Generally, the most important factor for a successful hot deformation process is the applied force, by which the maximum load of machine is not exceeded and die can work properly without causing any defects on the workpieces. Although some entrepreneurs have applied computational technologies and computer simulation techniques to their development step, but the metallurgical aspect and databases of material properties are still insufficient. The decisive parameters for the calculation are not only geometries of the component and boundary conditions such as temperature distribution, but certainly the material properties. In the hot forming industry, reliable experimental data describing deformation behaviour of material at hot working temperature and phase transformation is required. These material data are applied to the FE simulations in order to accurately predict and control the hot forming process. This study was aimed to investigate material properties with respect to the deformation behaviour and phase transformation behaviour of two carbon steels, AISI 1045 and AISI 1055. These steels are widely used in various applications, especially in the automotive industries. The phase transformation of the steels during continuous cooling after deformation at high temperature was examined by means of a dilatometry testing at various cooling rates with regards to the time duration between 11520 and 4 seconds in the $t_{8/5}$ period and was presented in the form of D-TTT diagram. Furthermore, the flow curves of materials at different

temperatures were determined. An attempt has been done to apply these determined material data in the FE simulations of a simple hot forging process. The primary results showed that it is possible to calculate the macroscopic process parameter such as punch load as well as the resulted microstructure development, DRX grain size, and hardnesses of any local areas of the deformed parts. In the future, parameter study of the model and validation with experiments will be carried out.

2 Experiments

The materials used in this work are AISI 1045 and AISI 1055 medium carbon steel. Their chemical compositions are shown in Table.1

Table 1: Investigated Materials

Steel	Mass content in %				
	C	Si	Mn	P	S
AISI 1045	0.44	0.28	0.89	0.013	0.011
AISI 1055	0.53	0.21	0.71	0.015	0.020

The entire experimental work was arranged in three examinations which are explained in detail as followed.

I. Deformation behaviour of two medium carbon steels, AISI 1045 and AISI 1055 was characterized at their hot working temperature region. Thereby, flow curves for both steels were determined in hot compression test on a deformation dilatometer machine type Baehr DIL805. A schematic illustration of the machine is presented in Figure 1. The testing temperatures were 1423 K, 1473 K and 1523 K while the strain rates were varied at 0.001, 1 and 10 s^{-1}. Specimens for the test were prepared according to the Rastegaev sample as a 15 mm height cylinder with a diameter of 10 mm. The silica (SiO_2) powder was used between surfaces of the specimen and Alumina (Al_2O_3) punch as lubricant to minimize the interfacial friction. A homogeneous deformation until a maximum strain of 1.2 is therefore possible. First, the specimen was placed in a vacuum chamber filled with inert gas. The inert gas was applied to prevent an oxidation on the sample surface during the process. The specimen was then heated up to the target temperatures by an induction coil integrating with water cooling. The temperatures were hold for 180 seconds before start upsetting in order to obtain a uniform temperature distribution on the sample. The sample was compressed with a constant strain rate until reaching a strain of 1 for every test conditions. During the compression data for force and displacement of the driving rod were recorded. Finally, the sample was cooled down to room temperature by an inert gas.

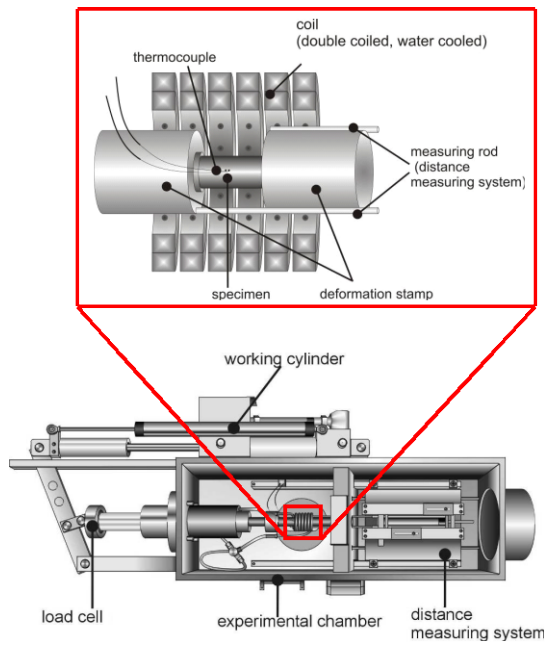

Figure 1: Deformation dilatometer machine.

II. Phase transformation during continuous cooling after deformation at high temperature was investigated on the same dilatometer machine with quenching module. The various cooling rates between $t_{8/5}$ time of 11520 and 4 seconds were carried out. These cooling rates correspond to the rates between 0.02 K/s and 66.32 K/s. The specimens were prepared in a cylindrical geometry with the same dimension as the previous tests. An alumina pad was attached at the tip of specimen holder to optimize heat transfer from the specimen to the specimen holder. This experiment was conducted in a vacuum chamber and under inert gas. The heating process also took place here by an inductor with double coiling. Thermocouple was used to measure and control the temperature on the sample for both investigations, namely, the hot compression and the continuous cooling dilatation test. The sample was firstly heated up to the austenitization temperature of a bit above 1523 K, held for 300 seconds and then fast cooled down to the deformation temperature

(test I) or continuously cooled down to room temperature with different cooling rates (test II) by inert gases (helium or argon). The applied cooling rates related to the length of time between 11520 and 4 seconds in the period of $t_{8/5}$ (from 1073 K to 773 K). During the cooling process, relative elongation of the specimen was recorded by two driving rods between the samples. This relative elongation was represented against temperature to identify when and which phase transformation has taken place. Figure 2 shows typical change in length during continuous cooling. Additionally, after cooling down to ambient temperature, the specimens were subjected to investigate the microstructure by optical microscope and measure the hardness value. The microstructural investigation was performed to characterize the occurring transformation as well as to determine the volume fraction of each phase in the microstructure. All these data were used for construction of the D-TTT diagram. The results of the hardness measurement were shown in Table 2 and 3 at the end of this paper for each material.

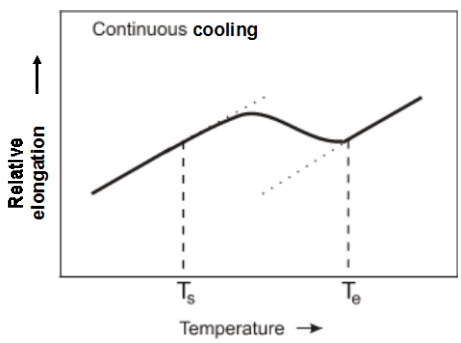

Figure 2: Typical change in length during continuous cooling.

Finally, constitutive analysis for examining strain rate sensitivity of material at high temperature was performed using the plastic flow curves obtained from the experimental data of the hot compression test.

3 FE simulations with cellular automata (CA)

3.1 *FE model*

In the FE simulations, the rigid-viscoplastic FEM was used, which is based on the rigid-viscoplastic variation principle. Usually, the governing equations for the solution of the mechanics of rigid-viscoplastic deformation do not consider the volume force and neglect the elastic deformation of the material and satisfy the equilibrium equation, the geometrical equation, volume constancy, and the material conforming to the Von Mises yield criterion [1]. Using the penalty function method to handle the condition of volume constancy, the energy function is expressed as follows:

$$\Phi = \int \sigma \bar{\varepsilon} dV + \frac{\alpha}{2} \int (\dot{\varepsilon} V)^2 dv - \int_{S_F}^{1} F_i U_i dS \qquad (1)$$

in which σ, $\bar{\varepsilon}$, $\dot{\varepsilon}$, α and F_i are the effective stress, effective strain rate, volume strain rate, penalty constant and external force, respectively. U_i is the velocity at the surface S_F and S_F is the area of the surface acted upon by the external force.

By the numerical analysis, effects of strain rate on the strain/stress distribution and microstructure evolution of AISI 1045 steel during hot compression process were investigated. Thermomechanical coupled FE calculations were performed using the FEM software package DEFORM-3D. The FE models of the billet sample at the initial and deformed state with a 50% reduction in height are shown in Figure 3 (a) and (b), respectively. These models correspond to the experimental setup of the dilatometry test. The boundary conditions in the FE-simulations and some thermal and physical properties of the tested material are described here. The friction at the interface between deformed block and tooling was assumed to be of a shear type and during the deformation a friction coefficient of 0.1 was applied because of the lubricated surfaces between the forging die and deformed block [2]. Due to the high temperature and large deformation taking place in the process, elastic deformation is negligible and all the dies are considered as rigid bodies [3]. The environment temperature is set to be as the room temperature of 20°C [4]. The convection coefficient to environment is 0.02 N/(smmC) [5]. The heat transfer coefficient between deformed sample and die is 5 N/(smmC) [6]. Due to the symmetry of the compression test, only one half of the block is simulated and used for the following discussion.

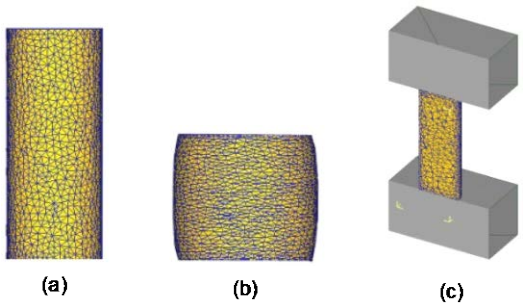

Figure 3: The used FE models: (a) initial billet (b) deformed block (c) symmetry of the specimens

3.2 *Microstructure evolution*

The development of microstructure was subsequently calculated by means of the Cellular Automata (CA) method considering the results from the macroscopic compression simulations. By this manner, any areas on the specimen can be chosen and investigated. Different types of recrystallization can take place before and after deformation. Here, the dynamic recrystallization was studied, which occurs during the deformation and when the strain exceeds a critical strain. The driving force is removal of dislocations. Before recrystallization begins or after recrystallization is completed grain growth can occur. However, the driving force is the reduction of grain boundary energy.

The dynamic recrystallization is a function of strain, strain rate, temperature, and initial grain size, which change with time. It has been stated that it is complicated to model the dynamic recrystallization concurrently during a forming process [7]. Instead, the dynamic recrystallization was computed in the step immediately after the deformation stops. Average temperatures and strain rates during the deformation period were used as input data of the equations.

1. Activation criteria [8]

The onset of DRX usually occurs at a critical strain $\varepsilon_c = \alpha_2 \varepsilon_p$. The parameter ε_p denotes the stain corresponding to the flow stress maximum:

$$\varepsilon_{p=} \alpha_1 \, d_0^{n_1} \dot{\varepsilon}^{m_1} \exp\left(\frac{Q_1}{RT}\right) + C_1 \qquad (2)$$

d_0 is the initial grain size, Q is the activation energy, R is the gas constant, T is the temperature in K, n and m is material data.

2. Kinetics

The Avrami equation is used to describe the relation between the dynamically recrystallized fraction X_{drex} and the effective strain ε.

$$X_{drex} = 1 - exp\left[-\beta_d \left[\frac{\varepsilon - \alpha_{10}\,\varepsilon_p}{\varepsilon_{0.5}}\right]^{k_V}\right] \qquad (3)$$

Where $\varepsilon_{0.5}$ denotes the strain for 50% recrystallization:

$$\varepsilon_{0.5} = \alpha_5 d_0^{n_5} \dot{\varepsilon}^{m_5} \exp\left(\frac{Q_5}{RT}\right) + C_5 \qquad (4)$$

α, β and k are the material data.

3. Grain Size

The recrystallized grain size is expressed as a function of initial grain size, strain, strain rate, and temperature

$$d_{rex} = \alpha_8 d_0^{n_8} \varepsilon^{m_8} \dot{\varepsilon}^{-m_8} \exp\left(\frac{Q_8}{RT}\right) + C_8 \qquad (5)$$
$$(if \quad d_{rex} \geq d_0 \, then \, d_{rex} = d_0)$$

4 Results

4.1 *Stress-strain relation and D-TTT diagram*

The stress-strain responses of the AISI 1045 and AISI 1055 steels determined in the hot compression test at different temperatures and strain rates were summarized in Figure 4 and 5, respectively. It was definitely found that higher stresses are established when temperature decreases and forming velocity increases. These compressive flow curves served as a significant input data in the FE calculations for predicting the necessary forging force of the process.

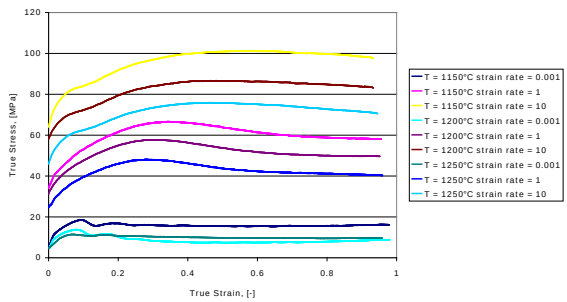

Figure 4: Stress-strain curves for steel AISI 1045 at different temperatures and strain rates.

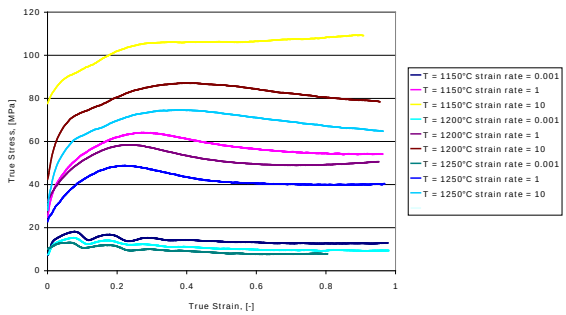

Figure 5: Stress-strain curves for steel AISI 1055 at different temperatures and strain rates.

In addition, the results from dilatometry investigation provide important information for characterizing the phase transformation of material during a continuous cooling. Interpreting the diagram of the relative elongation against temperature together with the microstructure analysis the conditions of time and temperature could be given, by which the transformation of different phases starts and completely finishes according to any cooling rates. The so-called deformation time-temperature-transformation diagram (D-TTT) was plotted by connecting each data of the determined transformation temperatures, microstructures, phase fractions, and hardnesses obtained from various cooling conditions. The D-TTT of AISI 1045 and AISI 1055 steels were represented in Figure 6 and 7, respectively. These D-TTT diagrams are a very useful tool for controlling and optimizing hot working and heat treatment process of steel. When cooling path of such process is known, approximate microstructure developed and hardness distribution in a workpiece undergoing that process can be obtained.

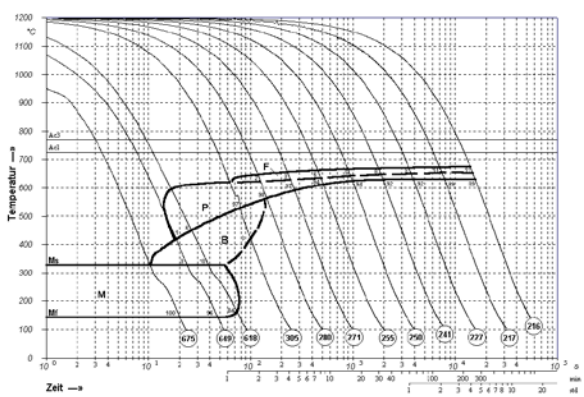

Figure 6: D-CCT diagram of steel AISI 1045.

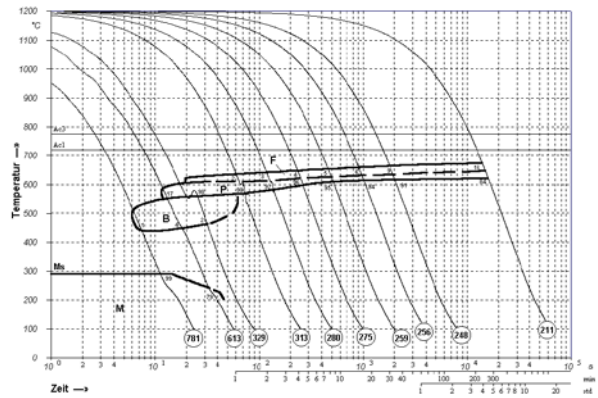

Figure 7: D-TTT diagram of steel AISI 1055.

4.2 *Numerical analysis*

Firstly, punch loads for different upsetting temperatures up to the strain according to a 50% reduction in height of the specimen were calculated from macroscopic simulation and are shown in Figure 8. It is obviously that punch force decrease at higher forming temperature. The compressive load could differ up to 2000 N for a temperature difference of 200°C at higher strain. In these calculations an isothermal condition was assumed similar to the dilatometry test, while the industrial forging is generally conducted under non-isothermal condition. The effect of non-uniform temperature distribution should be taken into account in order to achieve a successful forged part.

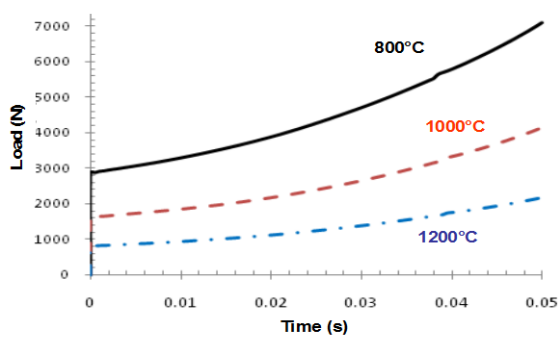

Figure 8: Punch load calculated for the upsetting temperatures of 800, 1000, and 1200°C for steel AISI 1045.

An attempt to simulate microstructure evolution in the hot deformed specimen using CA method has been done. To study the influences of deformation temperatures on the dynamic recrystallization was the first primarily aim of the micro-simulation. The calculation was performed for a tracking point from the middle of the billet where the highest strain was observed. Figure 9-11 show the distribution of recrystallized grains in size of this area at different forming temperatures of 800, 1000, and 1200°C with a constant strain rate of 10 s^{-1} and a deformation degree of 50 % (reduction in height). It is found that the grain size decrease as the working temperature is increased. The number of grains is definitely higher when material is upset at higher temperature.

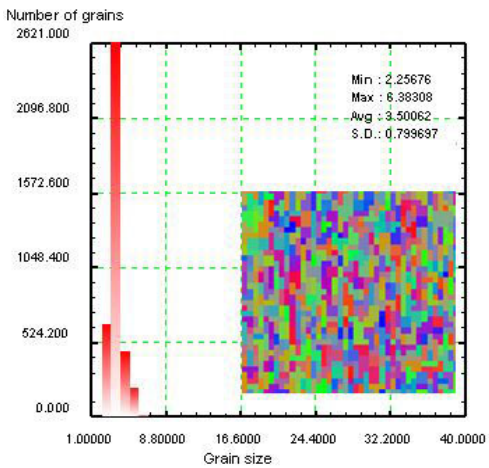

Figure 9: Distribution of grain size after recrystallization at a forming temperature of 800°C for steel AISI 1045 (averaged grain size ~ 3.50 μm)

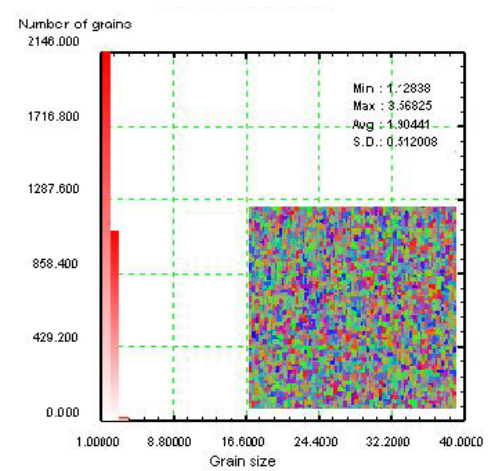

Figure 10: Distribution of grain size after recrystallization at a forming temperature of 1000°C for steel AISI 1045 (averaged grain size ~ 1.90 μm)

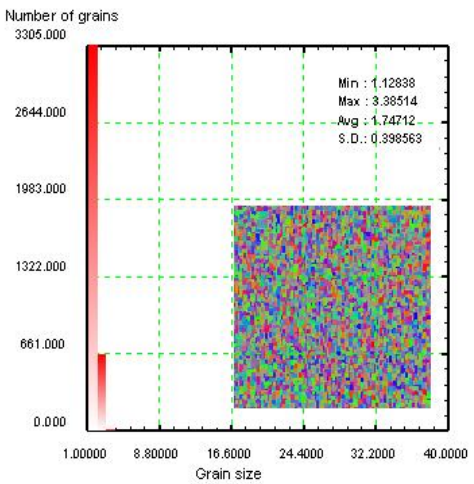

Figure 11: Distribution of grain size after recrystallization at a forming temperature of 1200°C for steel AISI 1045 (averaged grain size ~ 1.75 μm)

5 Discussion and Conclusion

It was observed that at the specified deformation temperature, when the strain rate is decreased, the material strength will decrease. However, at a constant strain rate, when the deformation temperature is increased, the material strength will decrease. The influence of strain rate on strength of material is stronger than that of the deformation temperature. The results at the strain rate of 10 s^{-1} show the highest strength value reached for all deformation temperatures, followed by the strain rate of 1 and 0.001 s^{-1}. The stress interval between 70 and 100 MPa was determined for strain rate of 10 s^{-1}, between 40 and 60 MPa for strain rate of 1 s^{-1} and between 10 and 15 MPa for strain rate of 0.001 s^{-1}. By performing at the strain rate of 0.001 s^{-1}, the material strength of specimens deformed at 1150, 1200 and 1250°C are almost in the similar level because of the effect of dynamic softening mechanism. The determined stress-strain responses reveal the influence of the dynamic softening. All results at strain rate of 0.001 s^{-1} show the similar stress level of about 15 MPa which is independent from the testing temperature. This observation could be the effect of the dynamic recrystallization. The same behavior was found for AISI 1055 steel. Therefore, in the forging process by which the strain rate is quite high, the deformation temperature has a significant effect on the strength of material and the corresponding punch load. The deformation

behaviour change dramatically when the temperature is changed. Thus, it is important to control the temperature in hot working process properly.

Regarding the determined D-TTT diagram microstructure of steel AISI 1055 cannot reach a 100% complete martensite fraction even after a very fast quenching since its M_f temperature is far below the room temperature. The regions of pearlitic and bainitic phase of AISI 1045 steel are larger than those of AISI 1055 steel. More martensite will be found in the microstructure of AISI 1045 steel for the same cooling rate. It can be seen that the diffusion-controlled phase transformation of AISI 1055 steel is stronger accelerated due to the deformation in comparison with AISI 1045 steel. Additionally, TTT diagram can be used as input data of FE simulation in order to predict phases existing in the microstructure of steel after hot forming.

In this work, experimental data as the compressive flow curves at different temperatures and strain rates, which were determined from the dilatometer machine, were given for the macroscopic simulations. The material parameters of the CA model are very important for calculating the microstructure evolution. To obtain more precise values of the recrystallized grain size for different temperatures these parameters should be determined from the results of dilatometry testing. For the results in this work parameters were mostly taken from the literatures. Nevertheless, it was shown that the CA approach incorporated in the FE programme can be applied to simulate the microstructure evolution during the hot upsetting process for AISI 1045 steel with consideration of the dynamic recrystallization mechanism. In the future, the microstructure prediction will be compared with results form metallography analysis in order to verify the averaged grain size and the developed phases.

Acknowledgments

The authors would like to thank the Iron and Steel Institute of Thailand and the Department of Ferrous Metallurgy, RWTH Aachen University for the fruitful experimental testing.

References

[1] Lin Y.C, Chen M.S. and Zhong J., 2008. Comput. Mater. Sci., 43 (4):1117-1122

[2] Dan W.J., Zhang W.G., Li S.H. and Lin Z.Q., 2007. Comput. Mater. Sci. 40: 101-107.

[3] Sommitsch C., Sievert R. and Wlanis T., Guenther B. and Wieser V., 2007. Comput. Mater. Sci. 39: 55-64.

[4] Liu J., Cui Z.S. and Li C.X., 2008. Comput. Mater. Sci. 41: 375-382.

[5] Lin Y.C., Chen M.S. and Zhong J., 2008. Comput. Mater. Sci., 43 (3): 470-477.

[6] Bouvier S., Alves J.L., Oliveira M.C. and Menezes L.F., 2005. Comput. Mater. Sci. 32 (3-4): 301-315.

[7] Sinczak J., Majta J., Glowacki M. and Pietrzyk M., 1998. Materials Processing Technology 80-81: 166–173

[8] DEFORMTM 3D Version 6.1 (sp1) User's manual Oct 10th 2007.

Table 2: Hardness of specimen AISI 1045 after dilatometry test with various cooling rate conditions

$\dot{\varepsilon}$,K/s	0.02	0.05	0.09	0.19	0.37	0.75	1.51	2.98	5.95	17.45	29.19	66.32
HV	216	217	227	241	250	255	271	280	305	618	649	675